Journal of Coastal Research	SI	54	127–140	West Palm Beach, Florida	Fall 2009

Geochemistry of Surficial Sediments from Lake Pontchartrain Resulting from the 1997 Opening of the Bonnet Carré Spillway

Jeffrey P. Waters†, Dale H. Easley‡, Scott E. Noakes§, and Shea Penland††

†Coastal & Hydraulics Laboratory
U.S. Army Engineer Research & Development Center
3909 Halls Ferry Road, Vicksburg, MS 39180, U.S.A.
Jeffrey.p.waters@usace.army.mil

‡Department of Natural and Applied Sciences
University of Dubuque
Dubuque, IA 52001, U.S.A.

§Center for Applied Isotope Studies
University of Georgia
120 Riverbend Road, Athens, GA 30602, U.S.A.

††Pontchartrain Institute for Environmental Sciences
339 CERM Bldg., Research & Technology Park, 2045 Lakeshore Drive, New Orleans, LA 70122, U.S.A.

ABSTRACT

WATERS, J.P.; EASLEY, D.H.; NOAKES, S.E., and PENLAND, S., 2009. Geochemistry of surficial sediments from Lake Pontchartrain resulting from the 1997 opening of the Bonnet Carré Spillway. *Journal of Coastal Research*, SI(54), 127–140. West Palm Beach (Florida), ISSN 0749-0208.

The Bonnet Carré Spillway is a flood-control structure that diverts Mississippi River water into Lake Pontchartrain during exceptionally high river stages. Because of elevated water levels in the Mississippi River in the spring of 1997, the Bonnet Carré Spillway was opened on March 17 and fully closed on April 18. The total volume of water discharged into Lake Pontchartrain was approximately 11.8 km^3, or two times the volume of the lake, and the total mass of sediment discharged into the lake was approximately 7.1×10^8 kg (780,000 US tons). In 1996, 757 surface sediment samples were collected in Lake Pontchartrain and were analyzed by x-ray fluorescence spectroscopy for major cation constituents. These same sites were revisited following the 1997 Mississippi River discharge event. Analysis of the 1996 and 1997 lake-bed sediment samples was accomplished utilizing fundamental statistical and graphical methods. Element concentration contour maps and variograms for the major cations illustrate meaningful differences between the pre- and postspillway sediment samples that are not readily apparent in the analysis of the descriptive statistics alone. Major cations exhibited significantly greater spatial continuity in the postspillway samples relative to the preceding year. The concentrations of aluminum and silicon in the postspillway sediments are considered to reflect, respectively, relative variations in clay and silt contribution to total sediment. The higher concentrations of magnesium in samples collected prior to the river diversion represent adsorption of magnesium onto exchange sites in surface sediments due to exposure to more saline waters.

ADDITIONAL INDEX WORDS: *Major cations, aluminum, silicon, potassium, calcium, iron, magnesium, sulfur, geostatistics, variogram, river diversion.*

INTRODUCTION

Lake Pontchartrain (Figure 1) is a shallow, estuarine lake (3.7 m average depth) with a surface area of 1631 km^2 and an average salinity of approximately 4 ppt (Sikora and Sikora, 1982). Holocene deposits in the Lake Pontchartrain Basin include transgressive nearshore or lagoonal–estuarine sediments (6000 to 4000 YBP), barrier shorelines deposits (~4000 YBP), and marginal deltaic sediments (~3000 YBP) deposited during the eastward progradation of the St. Bernard delta complex (Kindinger, Penland, and Williams, 2000a). These marginal deltaic deposits partially closed Lake Pontchartrain and isolated the lake from direct communication with the open waters of the Gulf of Mexico. Presently, saline water enters the eastern end of Lake Pontchartrain from the Rigolets and Chef Mentaur Pass. Tidal flow into (and out of) the lake is approximately 7500 m^3/s (Swenson, 1980a, 1980b). Saltwater intrusion also occurs through the manmade Inner Harbor Navigation Canal (IHNC) via the Mississippi River Gulf Outlet (MRGO) (Haralampides and McCorquodale, 2002). About 285 m^3/s of fresh water enters the lake primarily through streams, rivers, and bayous on the northern shore and through Lake Maurepas to the west (Figure 1).

The Bonnet Carré Spillway (Figure 1) is a flood-control structure that diverts Mississippi River water into Lake Pontchartrain during exceptionally high river stages. The 1325 ha spillway was completed in 1931 and is located about 19 km upstream from New Orleans on the left descending bank (Turner, Dortch, and Rabalais, 1999). The spillway was used to reduce floodwater heights in 1937, 1945, 1950, 1973, 1979, 1983, 1997, and 2008. Because of elevated water levels in the Mississippi River in the spring of 1997, the Bonnet Carré Spillway was opened on March 17 and fully closed on April 18 (Turner, Dortch, and Rabalais, 1999). The maximum peak flow rate of 6880 m^3/s was attained on March 27, 1997 and maintained through April 2, 1997. During the period in

DOI:10.2112/SI54-010.1.

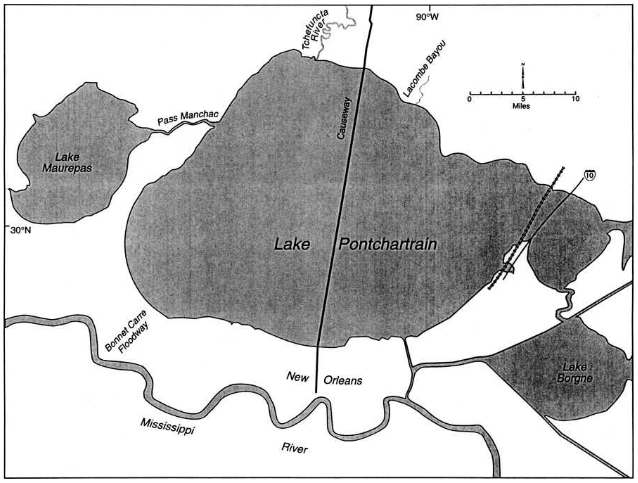

Figure 1. Lake Pontchartrain, Louisiana.

1997 that the spillway was open, the total volume of sediment-laden water entering Lake Pontchartrain was approximately 11.8 km^3, or two times the volume of the lake (Turner, Dortch, and Rabalais, 1999). At seven sampling stations along the Lake Pontchartrain Causeway in the center of the lake (Figure 1), the average total suspended sediment concentration peaked at approximately 70 mg/L during the spillway opening (Turner, Dortch, and Rabalais, 1999) and the total mass of sediment discharged into the lake was approximately 7.1×10^8 kg (780,000 U.S. tons). Additionally, satellite imagery (Figure 2) indicates that turbid Mississippi River water from the spillway was distributed throughout the lake by the end of April 1997.

Prior to the spillway opening, the USGS began a 5-year, multidisciplinary evaluation of the geology, geomorphology, coastal processes, and environmental quality of the Pontchartrain Basin for use by federal, state and local officials in coastal management and restoration planning (Kindinger, Penland, and Williams, 2000b). Lake-bed sediment characterization is an integral task of this Lake Pontchartrain study and to assist in this task, a rapid seafloor sediment-sampling and analysis system, developed by the Center for Applied Isotope Studies (CAIS) at the University of Georgia, was employed during September 1996 (CAIS, 1998). Seven hundred and fifty seven (757) surface sediment samples were collected in Lake Pontchartrain and analyzed by x-ray fluorescence spectroscopy for bulk chemical constituents. Following the spillway opening in 1997, CAIS repeated the survey in an effort to determine changes in lake-bed sediment chemistry. To build nonbiased elemental maps of the lake, sediment samples were collected during each survey of the lake bed on a predetermined, uniformly spaced grid (Figure 3). Both sample sets were analyzed for major cation (Al, Si, K, Ca, Fe, Mg, S, Ti, and Mn) and trace metal (Cu, Pb, Sr, Cr, Ni, Zr, Zn, Cd, Sn, Sb, and Ba) concentration by x-ray fluorescence spectroscopy (XRF). The purpose of this study is to evaluate the spatial variability of the major cation concentrations of sediment samples collected immediately preceding and subsequent to the spillway opening and to define the physical and chemical processes affecting spatial distribution.

METHODS

Continuous Sediment Sampling System (CS^3)

The CS^3 used a positive displacement pump mounted aboard a stainless-steel towed sled to deliver a continuous slurry of surficial sediment and water to a shipboard sample processor (CAIS, 1998). CS^3 samples were collected approximately every 1500 m along designated transects (Figure 3). The average ship speed between sampling stations was about 8 km/h. While cruising between stations, the CS^3 sled was towed high in the water column while pumping continuously, thus cleansing the sled, slurry hose, and shipboard processor, and minimizing the possibility of sample cross-contamination. As a sample station was approached, the ship speed was reduced, enabling the sled to descend to the lake bed. Upon contact with the sediment, a sediment slurry sample was transported through a hose connected to the shipboard processor.

Samples were collected by diverting a portion of the slurry that flows through the sample processor into a collection chamber. The slurry in the collection chamber was dewatered by suction and the remaining sediment, 50 to 150 mg, was deposited on a quartz-fiber filter. The nominal pore size of the quartz-fiber filter was 1.2 μm; however, sufficient filter clogging occurred during the collection process such that grains sizes smaller than the nominal pore size were collected on the filter. The sampling methodology was designed to concentrate the fine-grain clay and silt size fraction over the coarse-grain sand fraction relative to traditional surficial sediment sampling methodologies. Filter samples were dried at room temperature in a stainless-steel storage container and returned to the CAIS laboratory for XRF analysis.

The CS^3 was designed specifically for sampling sediments near the surface of the lake bed. It was not intended for deep penetration of the lake bed or representation of bulk composition of total lake-bed sediment. The fine-grained clays in the surface lake-bed sediment readily absorb anthropogenic metals, and by selectively sampling the surface sediment zone, an amplified signal can be detected from the lake bed. The technical specifications of the CS^3 are presented in Table 1.

XRF Analysis

The CS^3 filter samples were analyzed for elemental content using a Kevex 770 Analyst energy-dispersive XRF instrument. The CS^3 filter samples were analyzed "as is," *i.e.,* they were not subjected to any treatment prior to analysis. Filter samples were analyzed using standard CAIS procedures for XRF analysis, which included daily detector calibration checks using a stainless-steel reference disc and the measurement for an NIST 2704 standard along with each batch of 15 CS^3 samples (CAIS, 1998). Table 2 lists the target analytes and reporting units as well as the precision and accuracy values for the NIST 2704 standard.

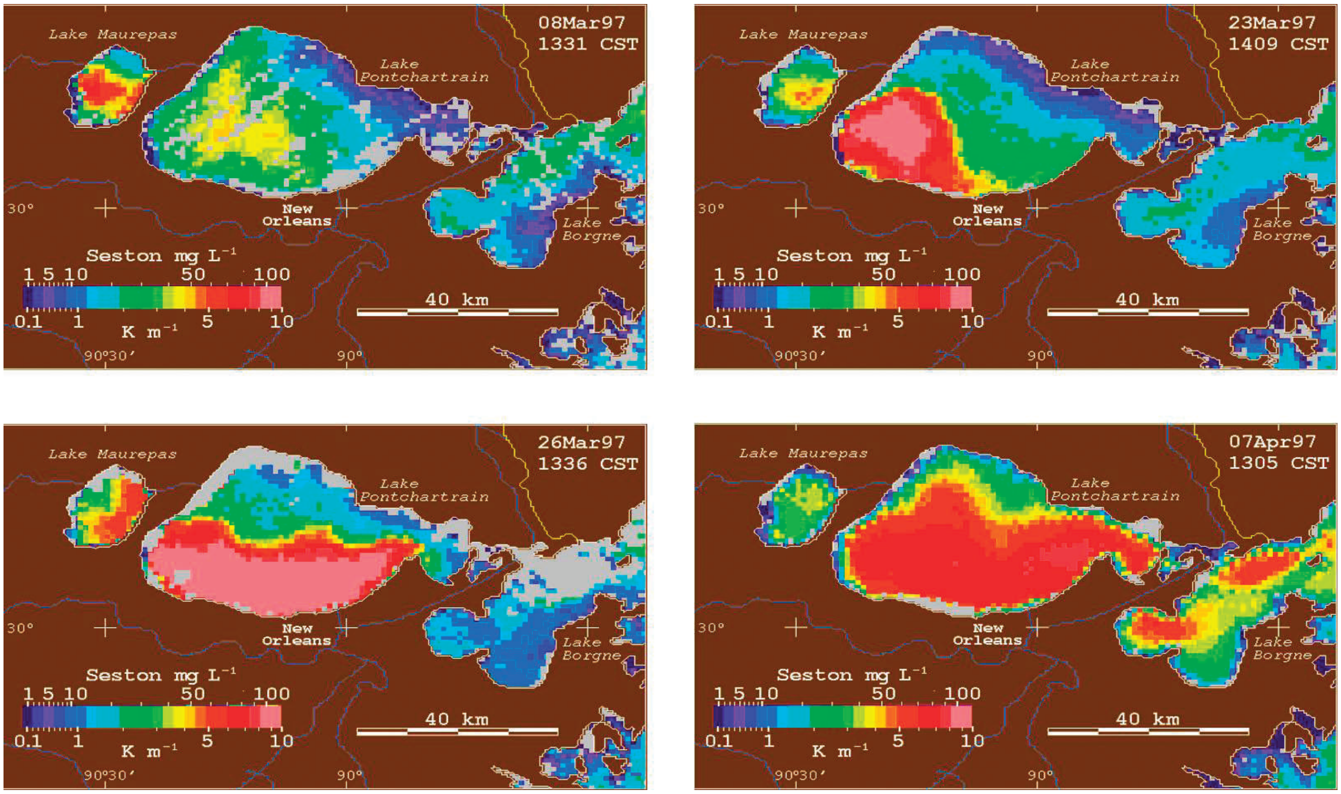

Figure 2. NOAA advanced very high resolution radiometer (AVHRR) satellite imagery for the periods immediately preceding and during the spillway opening. Inorganic suspended matter tends to create high reflectivity and the high reflectance patterns observed on March 23, March 26, and April 27 reflect particulate loadings from the spillway discharge. Dispersal patterns have been modified by wind-driven currents.

Each sample was weighed prior to analysis and typically ranged in weight from 40 to 200 mg. The weight variation was a function of the amount of fine-grained sediment suspended in the slurry pumped from the seafloor and collected on the quartz-fiber filter. The samples were then analyzed against a calibration curve derived from a set of standards close to, but not precisely equal to, the weight of the unknown. This method resulted in analytical totals that can vary from approximately 85% to 110%. To minimize the variation in analytical totals, we normalized the major oxide concentrations to an oxide total of 90%, allowing for the absence of Na_2O in the analyte list and the 5% to 10% structurally bound H_2O typically found in clay minerals in the estuarine environment. Elemental concentration values were reported as weight percent (wt%) and parts per million (ppm). The analyses resulting from the CS^3 Lake Pontchartrain survey were originally reported in Manheim and Hayes (2000).

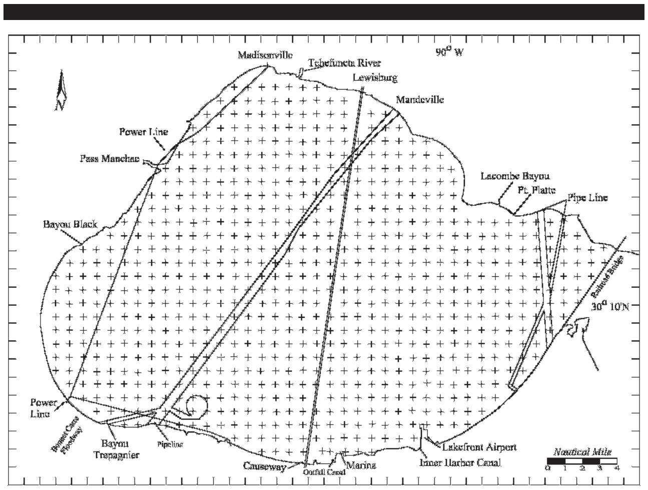

Figure 3. Lake-bed sediment sample locations for the 1996 and 1997 data sets.

Geostatistics

The term "geostatistics" was originally applied by Matheron (1963) to describe the theory and methods for estimating ore reserves from data that were spatially distributed throughout the ore body. In current usage, geostatistics is concerned with statistical theory and application for processes with continuous spatial variability, data that are intermediate between a truly random variable and one that is completely deterministic (Cressie, 1991). Fundamental to geostatistical analysis is the development of the variogram γ_h, which is a measure of the degree of spatial dependence

Table 1. *CS³ technical specifications.*

Analytical method	XRF (energy-dispersive x-ray fluorescence) spectroscopy
Data results	Parts per million (ppm)
	Weight percent (wt%)
Format	Hard-copy printout
Sampling interval	¾ nautical mile
Calibration test	NIST standards for XRF
Navigational method	Differential global positioning system (DGPS)
Operating range	
Penetration (sled)	2–10 cm
Ship speed (sampling)	2.5–3 knots
Ship speed (cruising)	8 knots
Sample	Sediment wafer on quartz-fiber filter
Sample size	31 mm
Sample weight	20–200 mg

Table 2. *Target analytes and detection limits.*

Element	Reporting Unit	Detection Limit	Accept/Reject
Al	wt%	0.0500	±25%
Si	wt%	0.0300	±25%
Mg	wt%	0.1400	±25%
K	wt%	0.0100	±25%
Ca	wt%	0.0100	±25%
S	wt%	0.0100	±25%
Fe	wt%	0.0012	±25%
Ti	wt%	0.0100	±25%
Mn	wt%	0.0019	±25%
Cu	ppm	4	±25%
Pb	ppm	10–14	±25%
Sr	ppm	9	±25%
Cr	ppm	14	±25%
Ni	ppm	7	±25%
Zr	ppm	11	±25%
Cd	ppm	10	±40%
Sn	ppm	10	±40%
Sb	ppm	10	±40%
Ba	ppm	10	±25%

between samples. If the spacing between samples is some distance Δh, the variogram is defined as:

$$\gamma_h = \frac{\sum (x_i - x_{i+h})^2}{2n} \qquad (1)$$

where x_i is a measurement of the continuous variable at location i, and x_{i+h} is another measurement taken at some distance h (Davis, 1986). For continuous data, if Δh is a small distance, the points being compared tend to be very similar and the value of the variogram is small. As the distance Δh is increased, the squared differences between points becomes larger until a distance is reached at which the points being compared are no longer spatially related and the value of γ_h becomes equal to the magnitude of the variance around the average value σ_0^2.

Some idealized models of the variogram are presented in Figure 4. Figure 4a represents a spherical model. For this model, the range a is the distance at which the variogram γ_h becomes equal to the sample variance (σ_0^2 = sill). For most geologic data, the variogram does not pass through the origin but assumes some nonzero value (Figure 4a). This is termed the "nugget effect" and is attributed to erratic behavior at very short distances so that γ_h goes from zero to the level of the nugget effect at a distance less than the sampling interval (Davis, 1986). The nugget effect includes sampling and analytical error as well as local heterogeneity. Figure 4b is a linear variogram. A failure of the sample variogram to flatten to a sill often indicates a trend in the data. A truly spatially uncorrelated random variable will have no spatial continuity, and the variogram will be a horizontal line equal to the sample variance (Figure 4c).

RESULTS

Preliminary analysis of the 1996 and 1997 lake-bed sediment samples was accomplished utilizing fundamental statistical and graphical methods. Descriptive statistics and frequency distributions for the major cations and trace elements were generated using Excel 97 software. Descriptive statistics for the 1996 (prespillway opening) and 1997 (postspillway opening) major cation concentrations are presented in Table 3. A positive difference represents an increase and a negative difference represents a decrease in that statistic from 1996 to 1997 (Table 3). Average values for the major cations in the pre- and postspillway sediment analyses demonstrate significant variability. The mean and median values for silicon, potassium, and manganese exhibit a slight increase from pre- to postspillway years, while calcium and iron demonstrate a moderate increase in the mean and median values. Aluminum and sulfur both exhibit a moderate decrease in the average values in the postspillway samples relative to the prespillway values, while magnesium demonstrates a strong decrease in both average values with the postspillway mean being equivalent to approximately 50% of the prespillway value.

Manheim and Hayes (2000) reported selected trace metal data for late 1970s Mississippi River suspended solids along with Lake Pontchartrain mean surficial sediment values. Within their trace metal concentration data set they also reported concentrations for the major cations Al and Fe. Manheim and Hayes (2000) report a mean weight percent value of 5.05 for Al concentration in Lake Pontchartrain surficial sediments while the results of this study report mean values of 7.07 and 6.61 for pre- and postspillway sediments, respectively (Table 3). As indicated previously, the CS³ sampling methodology concentrates the clay fraction relative to traditional surficial sediment sampling methodologies, and the marginal increase in Al concentrations reported here is considered consistent with an increase in clay content for these surficial samples. Similarly, pre- (4.02 wt%) and postspillway (4.77 wt%) Fe concentrations reported here exceed those (2.43 wt%) of Manheim and Hayes (2000). The partitioning of iron species (Fe^{3+}/Fe^{2+}) is not examined in this study; however, hydrated ferric oxides (Fe(III) oxyhydroxides) have been identified as major centers of ion adsorption in a variety of studies (Balistrieri and Murray, 1982; Laxen and Scholovitz, 1981; Lijkleme, 1980; Tipping, 1981) and would also be concentrated in the fine-grained fraction of the CS³ samples.

Element concentration contour maps and variograms for the major cations illustrate meaningful differences between

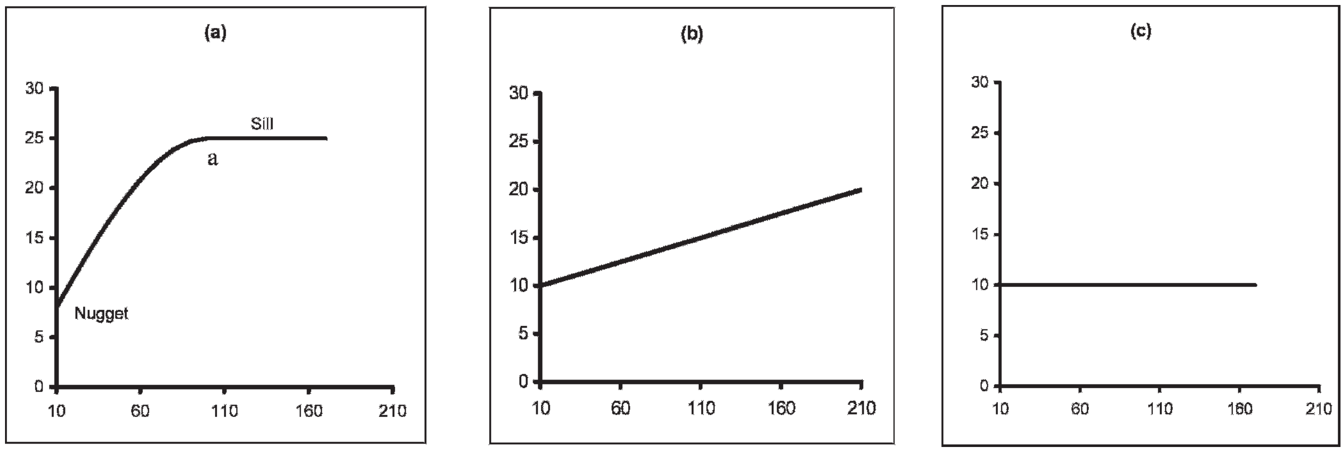

Figure 4. Idealized models of the variogram. An (a) exceptionally continuous variable modeled as a spherical variogram, (b) moderately continuous variable modeled as a linear variogram, and (c) a random variable with no spatial correlation.

the pre- and postspillway sediment samples that are not readily apparent in the analysis of the descriptive statistics alone. Aluminum is one of two major cations, sulfur is the other, that exhibits an increase in statistical variability in the postspillway samples relative to the preceding year (Table 3). Although sample variance is clearly greater in the 1997 data set, spatial variability is considerably lower in the postspillway sample set than in the 1996 data. In Figure 5b, aluminum concentration contour lines are generally continuous and enclose broad areas of a single concentration interval while the contour lines in Figure 5a are more discontinuous and generally enclose small, uneven areas of concentration intervals. The variograms of the aluminum concentration for the two data sets clearly document the differences in spatial variability preceding and subsequent to the spillway opening (Figure 5). The aluminum variogram for the prespillway sediments is essentially flat (spatially random) with individual values of γ_h clustered about the sample variance ($\sigma_0^2 = 0.766$, Table 3). The aluminum variogram for the postspillway sediments exhibits a high degree of spatial continuity (Figure 5d) and is modeled with a spherical variogram. The variogram sill (1.0) is approximately equal to the sample variance ($\sigma_0^2 = 1.158$, Table 3), and the range is consistent with a modeled value of 18,287 m (60,000 ft), indicating that aluminum concentrations are spatially related to a distance of more than 18 km (>11 miles). Figure 5b demonstrates that in addition to being spatially continuous, aluminum concentration contours delineate a clearly defined trend in the postspillway sediments; low aluminum concentrations are restricted to the margins of the lake while high aluminum concentrations (>7.0 wt%) occur only within a narrow zone in the center of the lake.

Table 3. *Descriptive statistics for surficial lake-bed sediments.*

Metal	Mean	Median	SD	Variance	Kurtosis	Skewness	Range
Al 96	7.07	7.13	0.875	0.766	0.002	−0.033	5.51
Al 97	6.61	6.73	1.076	1.158	0.474	−0.531	7.10
Change	−0.46	−0.40					
Si 96	29.35	29.46	1.332	1.774	0.056	−0.260	8.15
Si 97	30.10	29.94	1.314	1.727	0.211	0.458	9.53
Change	0.75	0.48					
K 96	1.73	1.67	0.424	0.180	0.587	0.838	2.50
K 97	1.88	1.88	0.242	0.058	−0.087	−0.193	1.51
Change	0.15	0.21					
Ca 96	0.38	0.36	0.149	0.022	0.443	0.817	0.91
Ca 97	0.53	0.51	0.141	0.020	6.691	1.737	1.22
Change	0.15	0.15					
Fe 96	4.02	3.74	1.161	1.347	2.153	1.311	7.13
Fe 97	4.77	4.77	0.833	0.693	−0.325	−0.078	4.85
Change	0.75	1.03					
Mg 96	1.89	1.74	0.941	0.886	2.025	1.222	5.76
Mg 97	0.96	0.95	0.358	0.138	15.413	2.20	4.45
Change	−0.93	−0.79					
Mn 96	0.24	0.21	0.160	0.026	0.850	1.000	0.86
Mn 97	0.26	0.25	0.125	0.016	0.928	0.651	0.90
Change	0.02	0.04					
S 96	0.97	0.86	0.160	0.026	0.849	1.000	0.86
S 97	0.63	0.57	0.330	0.109	68.835	6.392	4.95
Change	−0.34	−0.29					

Values are weight percent (wt%). The difference in the average values (mean and median) for an elemental pair (*e.g.,* Al 96 and Al 97) is reported in the row immediately following the records for each elemental pair.

The concentration contour maps and variograms for silicon also demonstrate a significant difference in spatial variability between pre-and postspillway sediments. Silicon concentrations are notably less heterogeneous in the postspillway sediments (Figure 6b) than in the sediments from the preceding year (Figure 6a). The variograms for the two sample sets confirm the differences in spatial variability. The variogram for the prespillway data set exhibits random behavior with γ_h clustered about the sample variance (1.774), while the data from the postspillway samples conform to a spherical model with the sill (1.6) approaching the sample variance (1.727) at a range of 18,287 m (60,000 ft). Figure 6b indicates that silicon concentrations in the postspillway sediments manifest a trend that is inverse to that of aluminum, with high silicon concentrations restricted to the periphery of the lake while low silicon values dominant the central portion of the basin.

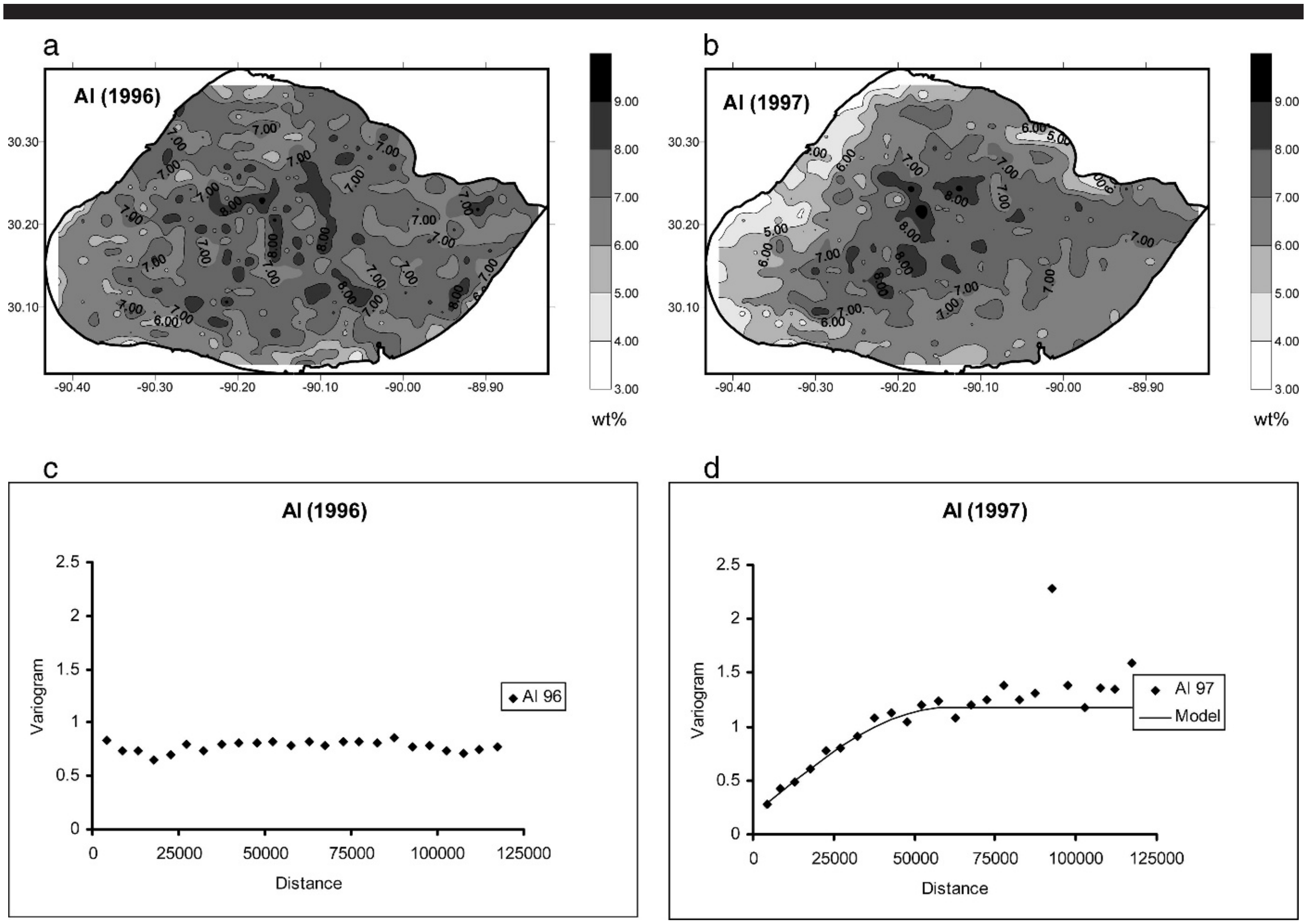

Figure 5. Aluminum concentrations (wt%) of surficial lake-bed sediments from (a) prespillway and (b) postspillway samples and variograms for aluminum from (c) prespillway and (d) postspillway sediments. The postspillway data are modeled with a spherical variogram and a sill of 1.0 with a range of 18,287 m (60,000 ft).

Potassium and calcium exhibit similar spatial relationships in the postspillway sediments relative to the prespillway samples. Contours are more continuous and generally enclose broad areas of a single contour interval in the postspillway samples while the 1996 data sets are much more heterogeneous (Figures 7 and 8). Variograms for sediments collected prior to the spillway opening illustrate random behavior and approach the sample variance of 1.8 for potassium and 0.022 for calcium. Variograms for potassium and calcium from the postspillway sample sets were both modeled with a spherical model to a range of 6100 m (20,000 ft) and a linear model to a range of 36,574 m (120,000 ft). A linear model implies a trend in the data, and this is consistent with the observations that potassium concentrations decrease from south to north in the postspillway sediments (Figure 7b) while calcium concentrations from the same samples generally decrease in a northerly direction (Figure 8b). The linear portion of each of these two variogram models exceeds the sample variance (potassium = 0.058 and calcium = 0.02) at approximately 19,811 m (65,000 ft), and it is unlikely that the spatial continuity of the metals exceeds 19,811 m.

The mean iron concentration of the postspillway sediments exceeds the prespillway samples by almost 20% of the prespillway mean. This is apparent in evaluating the gray-scale concentration contour map because the prespillway map is considerably darker than the 1997 map (Figure 9). Similar to the other major cations, the iron variogram for the prespillway sediments exhibits random behavior with γ_h clustered about the sample variance of 1.347. The iron variogram for the postspillway samples (Figure 9b) conforms to a spherical model with a range of 10,668 m (35,000 ft) and a sill at 0.72, consistent with the sample variance of 0.693 (Table 3).

In contrast to iron, the mean magnesium concentration of the postspillway sediments is much lower than the prespillway mean, equaling approximately 50% of the mean for magnesium from the preceding year. This is also apparent in Figure 10, which indicates much higher concentrations in the prespillway map (Figure 10a) than the postspillway map (Figure 10b) and also demonstrates that concentration contours are significantly more continuous for the postspillway data. In addition, the 1996 magnesium variogram (Figure 10c) exhibits random behavior with values widely distributed about the sample variance (0.886) while the postspillway magnesium variogram conforms to a spherical

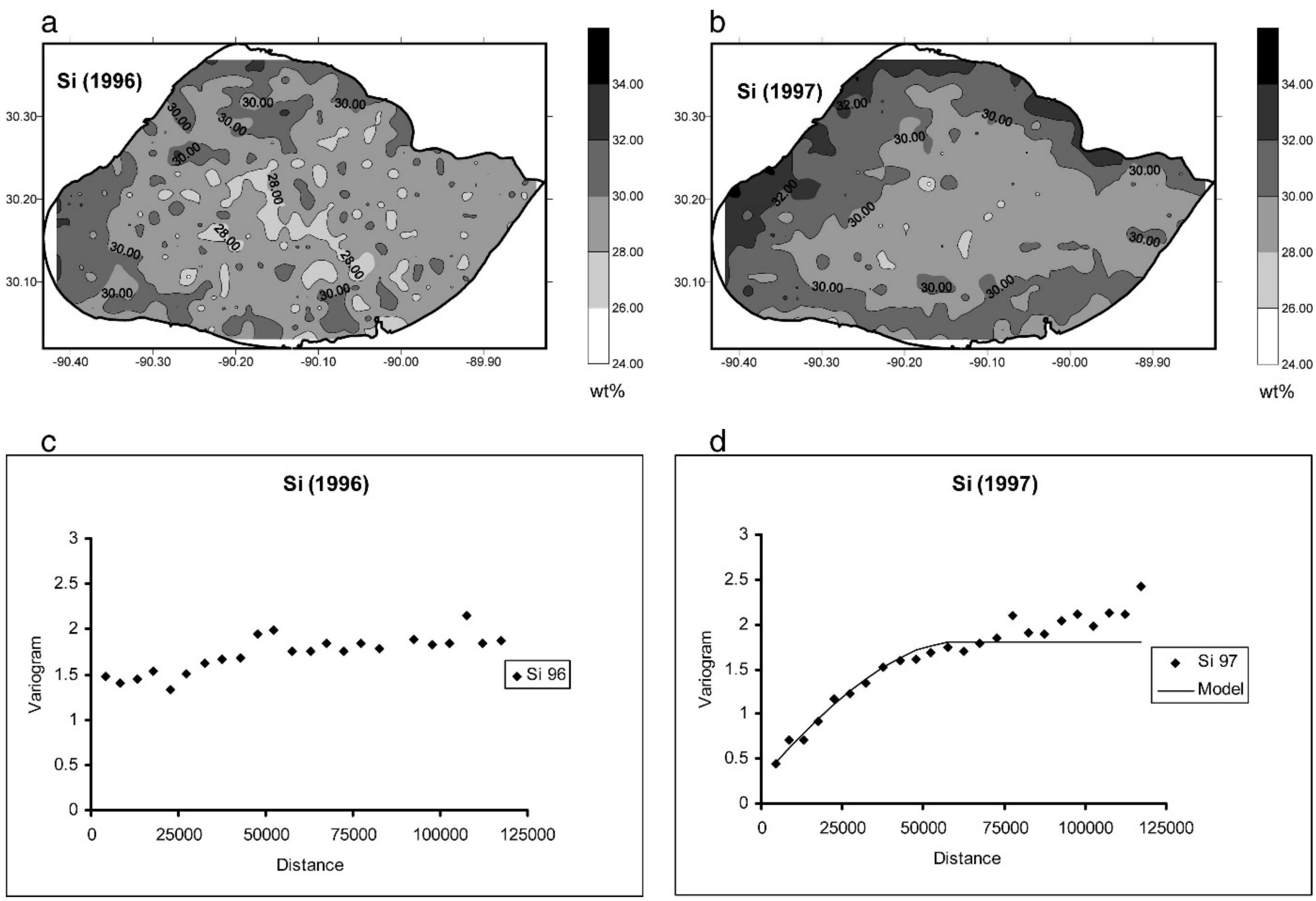

Figure 6. Silica concentrations (wt%) of surficial lake-bed sediments from (a) prespillway and (b) postspillway samples and variograms for silicon from (c) prespillway and (d) postspillway sediments. The postspillway data are modeled with a spherical variogram and a sill of 1.6 with a range of 18,287 m (60,000 ft).

model with a range of 13,715 m (45,000 ft) and a sill at 0.12, consistent with the sample variance ($\sigma_0^2 = 0.138$).

Sulfur concentrations from pre- and postspillway sample sets exhibit both spatial similarities and differences. The mean sulfur concentration (Table 3) is almost one-third lower in the postspillway sediments than the preceding year's samples, and that relationship is obvious in the concentration contour maps (Figure 11). In general, however, the sulfur concentration increases from west to east in both the pre- and postspillway sediment sets. The sulfur variograms express this linear trend via moderately continuous, increasing trends in γ_h with increasing interval distance. The average sample variance is considerably lower in the prespillway sediments ($\sigma_0^2 = 0.026$) relative to the postspillway samples ($\sigma_0^2 = 0.109$). In both years, high sulfur concentrations occur along the southern periphery of the lake with the highest concentrations adjacent to the Bonnet Carré Spillway in the southwest corner of the lake.

DISCUSSION

The 1997 diversion of Mississippi River water into Lake Pontchartrain resulted in the discharge of 7.1×10^8 kg (780,000 U.S. tons) of sediment into the lake (Turner, Dortch, and Rabalais, 1999). Assuming an average sediment density of 2.65 g/cm^3, if the material were distributed uniformly over the lake bed, it would form a blanket deposit 1.8 cm thick. Certainly the Mississippi River sediment was not deposited uniformly; however, the AVHRR imagery acquired during the diversion event (Figure 2) indicates that sediment-laden water was distributed throughout almost the entire lake within 3 weeks of the opening of the spillway. The Mississippi River diversion also transferred a significant amount of nutrients (nitrogen and phosphorous) into Lake Pontchartrain, which eventually resulted in a massive bloom of cyanobacteria (principally *Anabaeba* spp. [Turner, Dortch, and Rabalais, 1999]) in the lake in late June and July of 1997. The onset of the algae bloom was delayed more than 3 months as a result of light limitations resulting from exceptionally high turbidity in the lake during April, May, and June 1997 (Turner, Dortch, and Rabalais, 1999). Turbidity levels did not return to seasonal average values until July of 1997, suggesting that sediment derived from the Mississippi River remained dispersed in the water column (and throughout the lake) for up to 3 months after the spillway closure. Therefore,

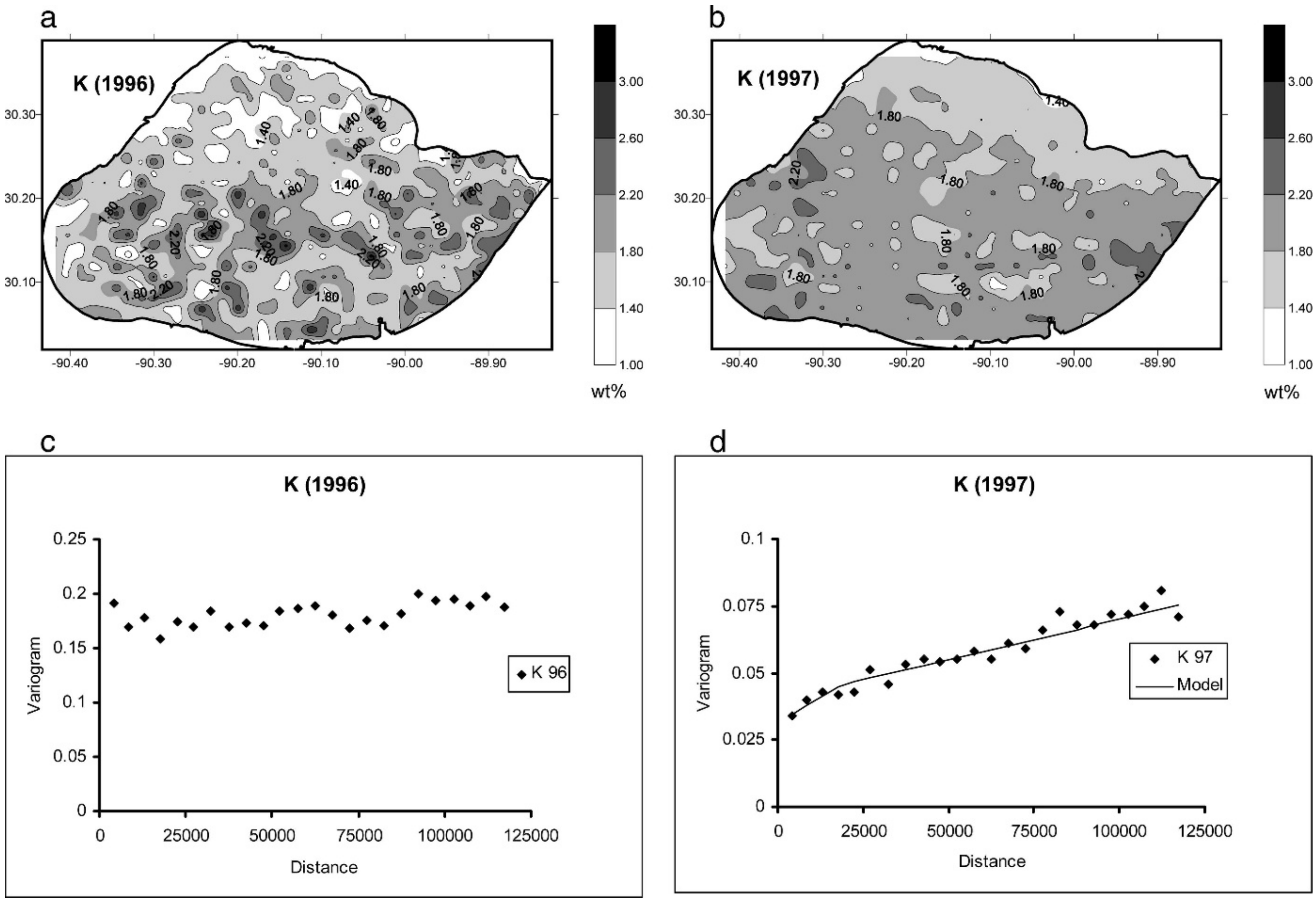

Figure 7. Potassium concentrations (wt%) of surficial lake-bed sediments from (a) prespillway and (b) postspillway samples and variograms for potassium from (c) prespillway and (d) postspillway sediments. The postspillway data are modeled with a spherical model to a range of 6100 m (20,000 ft) and a linear model to a range of 36,574 m (120,000 ft).

it is reasonable to suspect that much of the lake bed was subject to sediment deposition during this event.

Silicon and Aluminum

The elemental concentration contour maps and geostatistical analysis clearly suggest that the spillway opening produced a marked change in the spatial variability of major cation concentrations following the discharge event relative to the antecedent conditions. As a first-order approximation, it is assumed here that elevated silicon concentrations can be considered as an indicator of high concentrations of silt (quartz) while elevated aluminum concentrations can be considered a surrogate for clay. Figures 5 and 6 reveal a very high degree of spatial continuity for silicon and aluminum in the postspillway sediments with concentrations spatially related to a distance of 18,287 m (60,000 ft). The concentration contour maps for silicon and aluminum reveal a reciprocal relationship for the postspillway sediments: (1) silicon (silt) is concentrated around the periphery of the lake, especially the western boundary, and relatively depleted in the center of the lake and (2) aluminum (clay) is enriched in the central portion of the lake and depleted around the periphery.

Signell and List (2002) evaluated circulation patterns, wind-generated waves, and sediment resuspension in Lake Pontchartrain by modeling and measuring wind-induced waves and associated bottom currents and by measuring the resuspension and transport of sediment that occurs under a variety of conditions. They developed a three-dimensional circulation model and identified three primary mechanisms controlling the long-term transport of water in Lake Pontchartrain: (1) forcing by river water from the north shore that enters the lake primarily through Lake Maurepas and produces weak, seasonal eastward flow, (2) sea level fluctuations in Mississippi Sound that generate reversing currents in the eastern portion of the lake but do not affect the central and western portions of the lake, and (3) direct forcing by wind blowing over the surface of the lake, which creates a two-gyre pattern with relatively strong downwind currents near the coast and a return flow current directed against the wind in the middle of the lake. The magnitude of the currents varies with the wind speed, with 15 knots of wind generating downwind currents of 10 km/d along the coast and a return

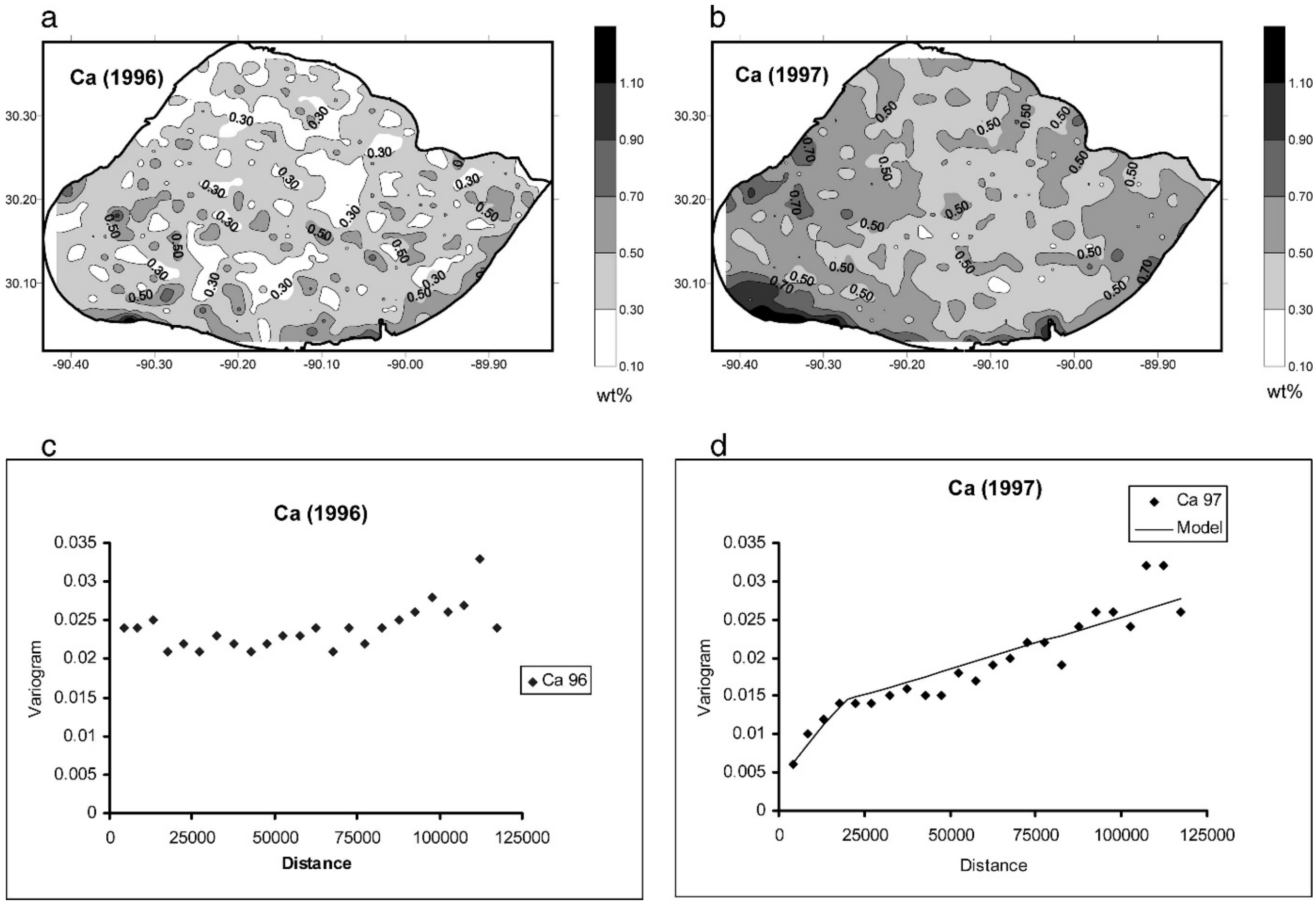

Figure 8. Calcium concentrations (wt%) of surficial lake-bed sediments from (a) prespillway and (b) postpillway samples variograms for calcium from (c) prespillway and (d) postspillway sediments. The postspillway data are modeled with a spherical variogram to a range of 6100 m (20,000 ft) and a linear model to a range of 36,574 m (120,000 ft).

flow current of about 5 km/d in the deeper regions of the lake (Signell and List, 2002). Current vectors are directed inward and are significantly lower in the central portion of each circulation cell. Haralampides *et al.* (2000) modeled saline water inflow and outflow during and preceding the 1997 Bonnet Carré Spillway diversion and confirmed the two-gyre wind-driven circulation pattern for Lake Pontchartrain.

The 1997 sediment samples for this project were collected in August and September, within 3 months of the time that lake turbidity levels returned to normal seasonal averages and therefore shortly after deposition of the sediments derived from the Mississippi River. Figure 12 is a quartile concentration map for silicon and aluminum concentrations from the postspillway sediment samples. It demonstrates that silicon, a surrogate for the silt fraction, is concentrated along the periphery of the lake, while aluminum, a proxy for the fine-grained clay fraction, is concentrated in the central portion of the lake. The predominant gradient wind during the summer in southern Louisiana is from the southeast and is generally only briefly interrupted by local thunderstorm activity. According to the two-gyre circulation model, this wind pattern would establish two circulation cells in the lake with the strongest currents along the shoreline and oriented downwind, a return flow current in the center of the lake oriented upwind, and significantly diminished currents directed toward the center of each circulation gyre. The sediment distribution patterns suggested by Figure 12 are consistent with the two-gyre circulation model. Silicon (silt) is concentrated along the periphery of the lake, especially the western and northern borders. The high concentrations in these regions are considered to reflect proximity to the source (Bonnet Carré Spillway) location in the southwest corner of the lake. Although silicon concentrations are somewhat lower in the southern and southeastern portions of the lake (Figure 12), most samples in these regions fall in the 50%–75% quartile. Aluminum (clay) is concentrated in the center of the lake and greatly diminished along the periphery where wind-generated currents would be strongest. In fact, the bimodal spatial distribution of the 75%–100% aluminum quartile suggests clay deposition in the center of two circulation cells. The lack of similar distribution patterns for sediment samples representing antecedent conditions is

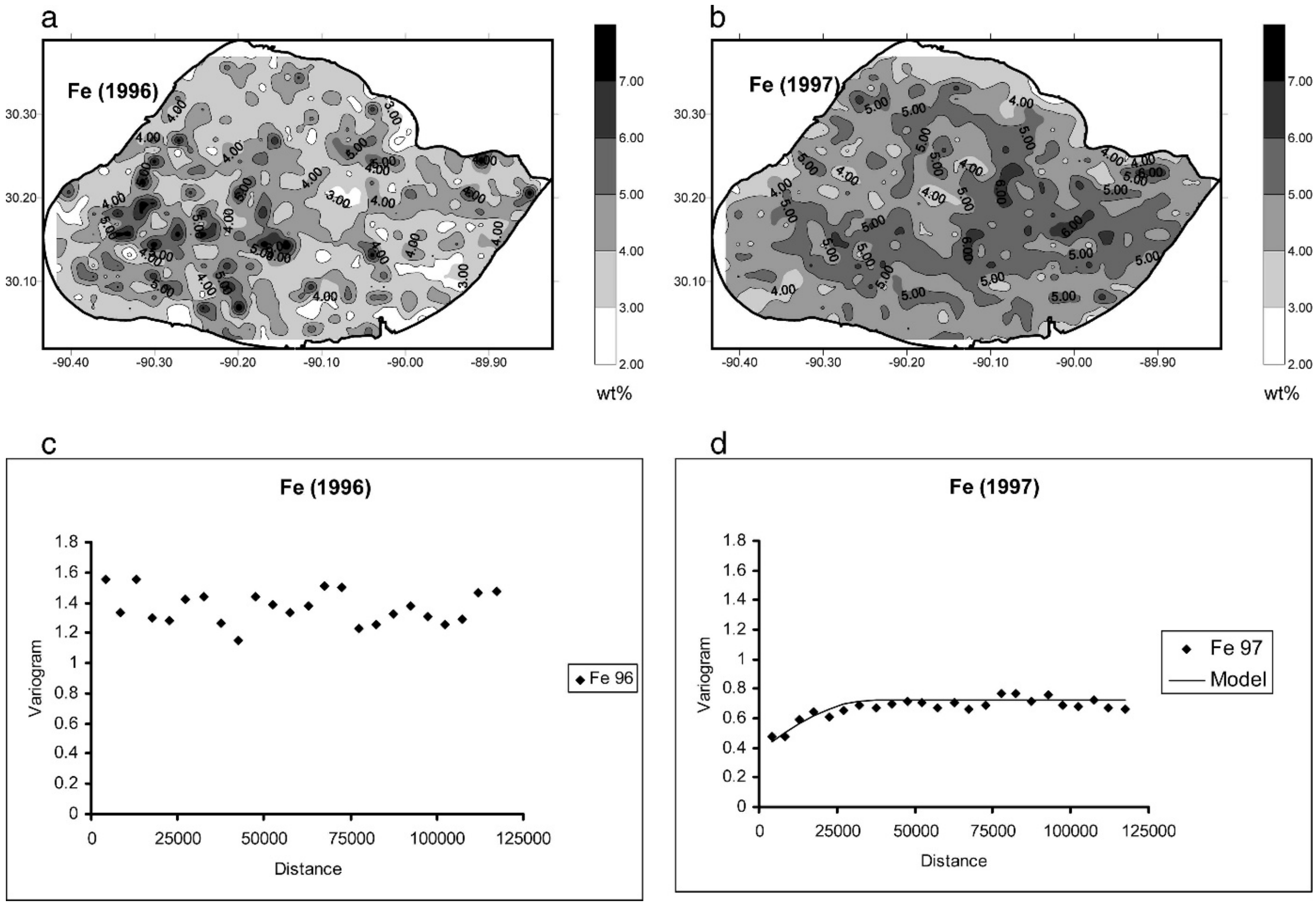

Figure 9. Iron concentrations (wt%) of surficial lake-bed sediments from (a) prespillway and (b) postspillway samples and variograms for iron from (c) prespillway and (d) postspillway sediments. The postspillway data are modeled with a spherical variogram and a sill of 0.72 with a range of 10,668 m (35,000 ft).

considered to reflect sediment mixing due to divergent wind patterns with winter frontal passages and the effects of mixing due to tidally generated currents.

Magnesium

Relative to the other major cations, the descriptive statistics for postspillway magnesium concentrations exhibit the largest divergence from prespillway values. The postspillway mean is less than half of the prespillway value, and the variance in the 1997 sediments is less than a quarter of the variance in the preceding year's samples. This difference in the statistics of central tendency is especially apparent in the histogram (Figure 13), which shows that the prespillway concentrations are uniformly greater than the postspillway mean and median. Although the magnesium variogram for the prespillway sediments does not indicate any degree of spatial continuity, it is apparent from Figure 9 that magnesium in the prespillway sediments is concentrated in the southeast quadrant of the lake.

Poirrier (1978) initially identified salinity stratification in southern portions of Lake Pontchartrain and attributed the increased bottom salinities to the IHNC. The IHNC is connected to the MRGO, a manmade navigation channel dredged through the marshes of southeast Louisiana to the Gulf of Mexico. The IHNC/MRGO is a very efficient hydrologic conduit for the transport of highly saline waters into Lake Pontchartrain. This saltwater intrusion into the lake produces salinity stratification and episodic hypoxia (dissolved oxygen <2 ppm). Porrier, Abadie, and Franze (2000) have documented a 250-km^2 area in the southeast portion of the lake that is devoid of large (>20 mm) *Rangia cuneata* clams due to episodic hypoxia. This same area was previously shown to be affected by saltwater intrusion (Schurtz and St. Pe, 1984) and is identified in Figure 14. Georgiou, McCorquodale, and Haralampides (2000) have sampled vertical profiles in this area for dissolved oxygen (DO) and salinity, and reported bottom salinities in excess of 20 ppt and DO values less than 1 ppm.

Comparison of Figures 9 and 14 indicates that the area of low DO (and high salinity) in the southeast portion of the lake is coincident with the area of high magnesium concentration in the prespillway sediments. Although magnesium in Lake Pontchartrain sediments may occur as a minor primary

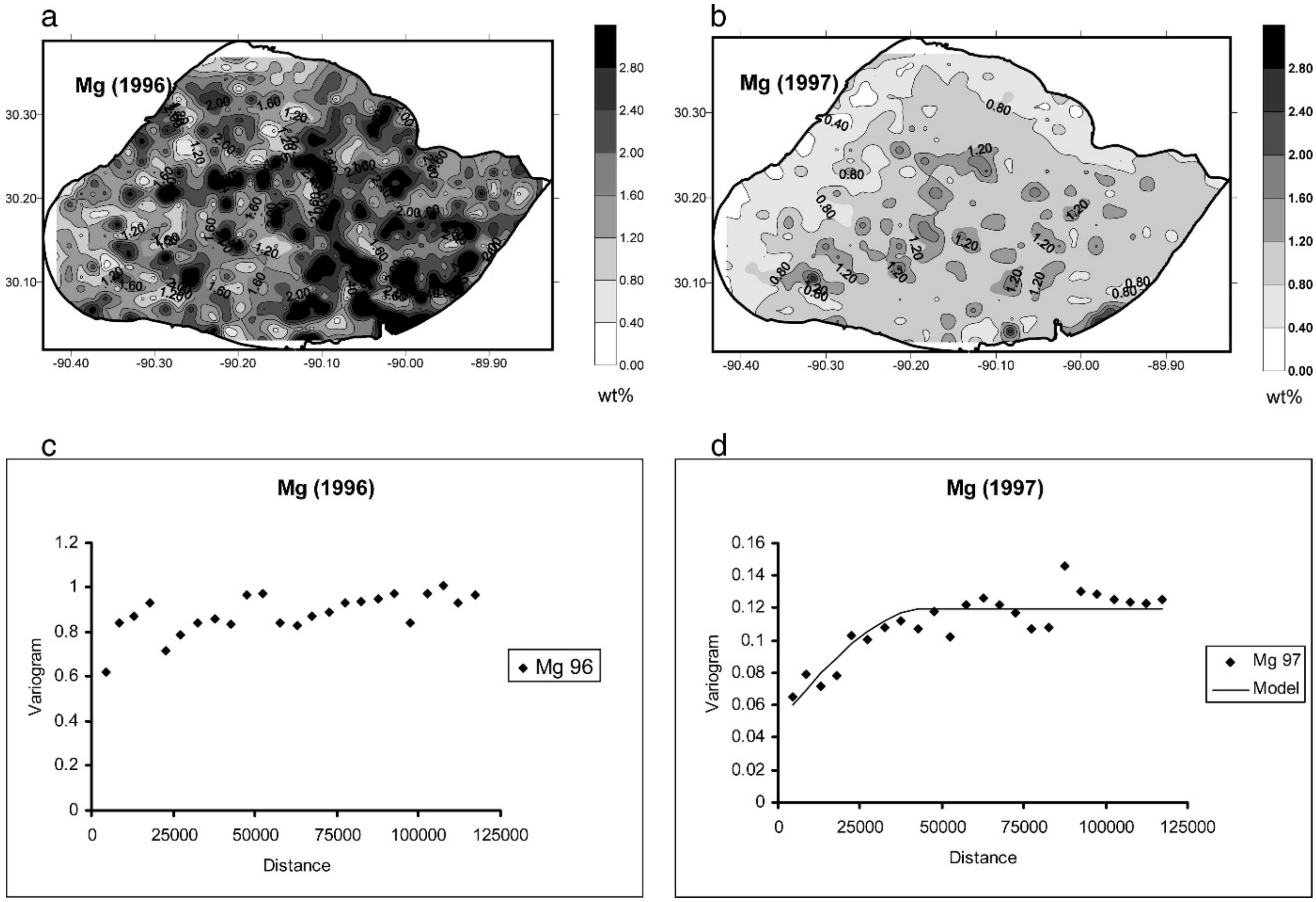

Figure 10. Magnesium concentrations (wt%) of surficial lake-bed sediments from (a) prespillway and (b) postspillway samples and variograms for magnesium from (c) prespillway and (d) postspillway sediments. The postspillway data are modeled with a spherical variogram and a sill of 0.12 with a range of 13,715 m (45,000 ft).

constituent of smectite, chlorite, or vermiculite clays structurally bound in the octahedral coordination site, it most likely occurs predominantly as a hydrated polar cation adsorbed onto the surface (exchange sites) of any of a number of fine-grained particles. Clay minerals in freshwater have their exchange sites occupied chiefly by calcium. When these clays encounter seawater, the calcium is replaced by sodium, potassium, and magnesium, and the net effect is to remove sodium, potassium, and magnesium from seawater and supply calcium to seawater (Drever, 1982). The much higher concentrations of magnesium in the prespillway sediments represent adsorption of magnesium onto exchange sites in surficial sediments that result from exposure to more saline waters. That potassium does not exhibit a similar relationship to magnesium in these sediments may be because potassium occurs primarily as an interlayer cation in high charge micas (illites) and is not readily available for ion exchange reactions. Sodium was not measured in these sediments, and calcium is moderately depleted in prespillway sediments relative to the freshwater 1997 samples, consistent with ion exchange of calcium for magnesium.

Sulfur

Like magnesium, sulfur is also depleted in the postspillway sediments relative to the preexisting conditions (Figure 11). Sulfide mineralization is prohibited in oxic conditions, and the low concentrations of sulfur in the postspillway sediments are consistent with their oxygenated, freshwater source. Highest sulfur concentrations in the prespillway sediments occur adjacent to the shoreline, especially in the southeastern and southwestern portions of the lake (Figure 11). As stated previously, the southeastern area is subject to low levels of DO in the bottom waters, which would promote precipitation of sulfur-bearing minerals. In addition, these areas of the lake are adjacent to fresh and intermediate marsh vegetation and receive organic detrital matter as normal input to the surficial sediments. Precipitation of sulfur-bearing minerals requires dissimilatory reduction of oxidized sulfur species (sulfate and sulfite, for example) through bacterial reduction. The bacteria involved in the reduction reaction are heterotrophs and require organic matter for energy transfer (Langmuir, 1997). The elevated sulfur concentrations along

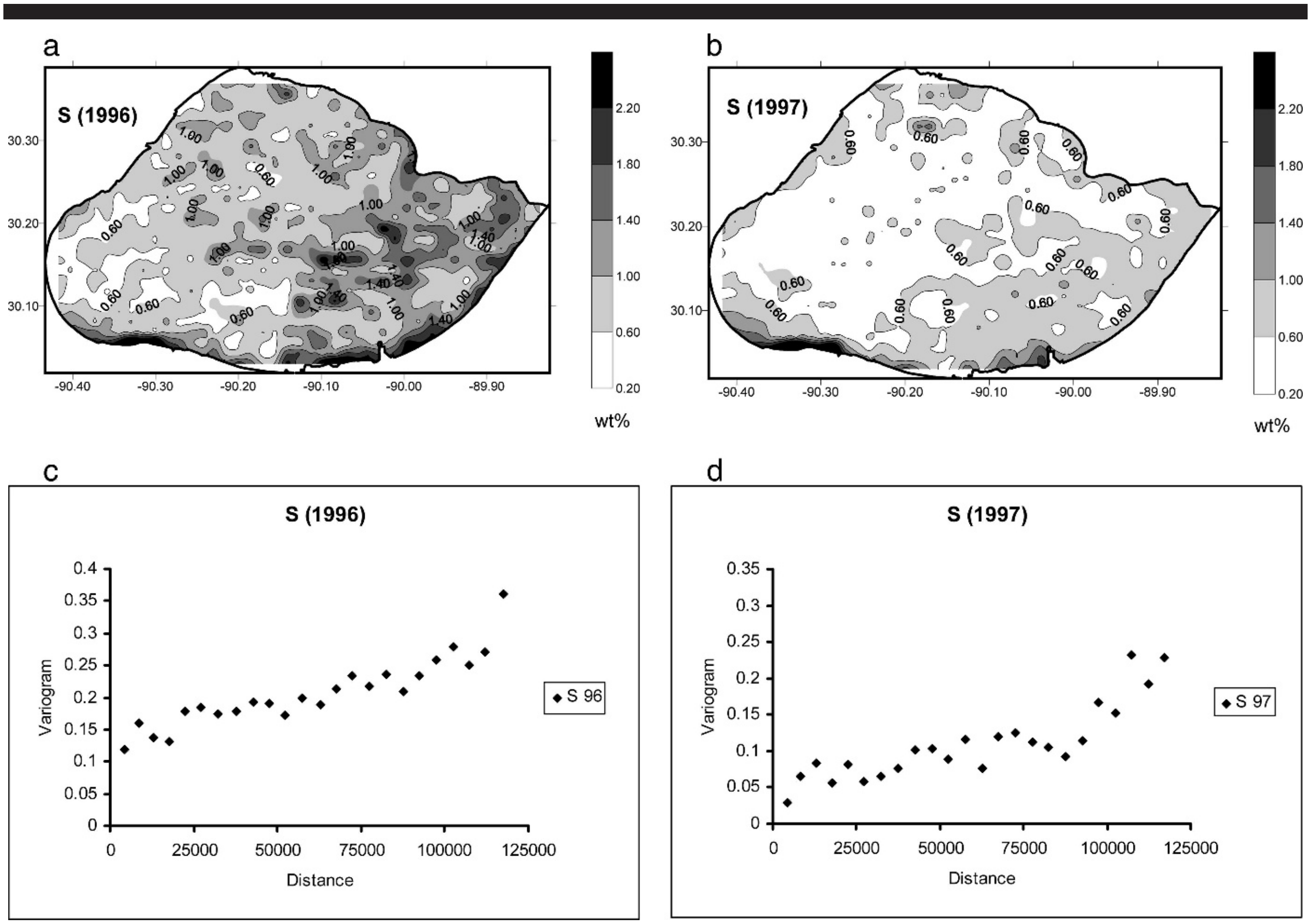

Figure 11. Sulfur concentrations (wt%) of surficial lake-bed sediments from (a) prespillway and (b) postspillway samples and variograms for sulfur from (c) prespillway and (d) postspillway sediments.

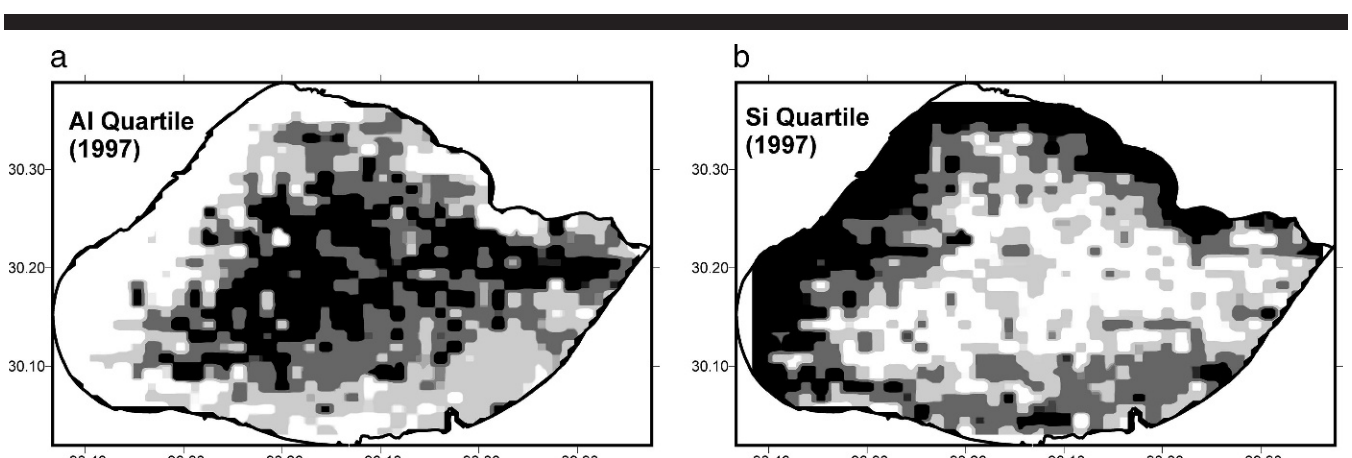

Figure 12. Aluminum and silicon quartile concentration maps for postspillway sediments. Aluminum is concentrated in the center of the lake while silicon is concentrated along the periphery of the lake consistent with the two-gyre circulation model of Signell and List (2002).

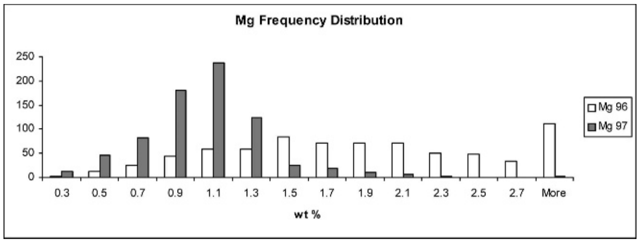

Figure 13. Magnesium frequency distributions for prespillway (1996) and postspillway (1997) sediments.

the southern periphery of the lake in the prespillway sediments likely reflect high inputs of detrital organic material in these areas. The elevated concentrations of sulfur in the vicinity of the Bonnet Carré Spillway in the postspillway sediments are the result of high inputs of detrital organic matter from the spillway structure following the cessation of the diversion event.

CONCLUSIONS

The 1997 diversion of Mississippi River water into Lake Pontchartrain resulted in the discharge of almost 7.1×10^8 kg of river-derived sediment into the lake. The spatial and statistical analyses of the bulk chemistry of sediment samples collected immediately preceding and following the diversion support several conclusions. First, all major cations exhibited significantly greater spatial continuity in the postspillway samples relatively to the preceding year. The 1996 samples represent antecedent conditions and reflect sediment mixing due to numerous frontal passages. The 1997 samples were collected shortly after deposition and reflect a single depositional event under relatively constant climatic conditions that affected the entire lake. Second, concentrations of aluminum and silicon in the postspillway sediments are considered to reflect, respectively, relative variations in clay and silt contribution to total sediment. The spatial continuity and concentration trends for aluminum and silicon support deposition in a two-gyre circulation pattern consistent with the hydrodynamic modeling of Signell and List (2002) and Haralampides *et al.* (2000). Third, magnesium is present in much higher concentrations in the prespillway sediments and the highest concentrations are concurrent with areas of known high bottom salinities. The higher concentrations of magnesium in prespillway sediments represent adsorption of magnesium onto exchange sites in surface sediments due to exposure to more saline waters.

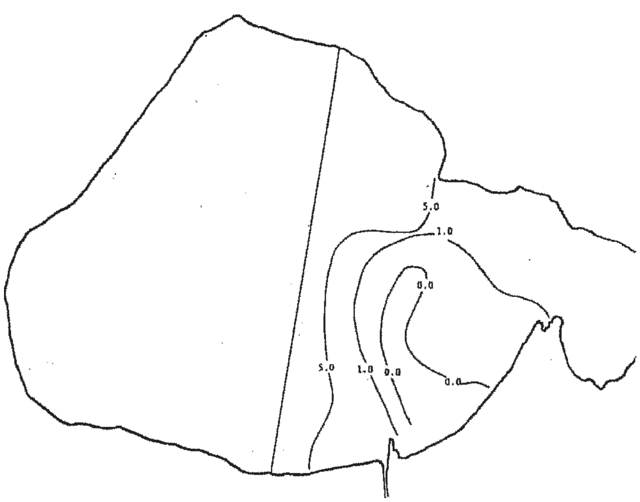

Figure 14. Contours of dissolved oxygen (DO) in Lake Pontchartrain bottom waters indicating area in the southeast portion of the lake with low DO values resulting from saltwater intrusion through the Inner Harbor Navigation Canal (modified from Schurtz and St. Pe, 1984).

ACKNOWLEDGMENTS

The authors would like to thank the U. S. Geological Survey and the Lake Pontchartrain Basin Foundation for providing the funding for the sediment sampling and analyses.

LITERATURE CITED

Balistrieri, L.S. and Murray, J.W., 1982. The sorption of Cu, Pb, Zn, and Cd on goethite from major ion seawater. *Geochimica et Cosmochimica Acta*, 46, 1253–1265.

CAIS (Center for Applied Isotope Studies), 1998. Areal (*sic*) Mapping of Surficial Sediment Metals at Lake Pontchartain, Louisiana. Final report submitted to the Lake Pontchartrain Basin Foundation. Center for Applied Isotope Studies. 87p.

Cressie, N., 1991. *Statistics for Spatial Data*. New York: John Wiley, 900p.

Davis, J.C., 1986. *Statistics and Data Analysis in Geology*. New York: John Wiley, 646p.

Drever, J.I., 1982. *The Geochemistry of Natural Waters*. Upper Saddle River, New Jersey: Prentice-Hall, 388p.

Georgiou, I.; McCorquodale, A., and Haralampides, K., 2000. Salinity and dissolved oxygen stratification in Lake Pontchartrain and the vicinity of the Inner Harbor Navigation Canal. Fifth Bi-Annual Basics of the Basin Research Symposium. Abstracts with Program. (New Orleans, Louisiana, Pontchartrain Research Committee), Abstracts with Program, pp. 28–32.

Haralampides, K. and McCorquodale, A., 2002, Wind-induced lake circulation patterns (N, S, E, W). *In:* Penland, S., Beall, A., and Kindinger, J. (eds.), *Environmental Atlas of the Lake Pontchartrain Basin*. New Orleans, Louisiana: Lake Pontchartrain Basin Foundation, U.S. Geological Survey Open File Report 002-206. CD-ROM available at http://pubs.usgs.gov/of/2002/of02-206/phy-environment/n-wind-circulation.html (accessed September 16, 2009).

Haralampides, K.; McCorquodale, A., and Georgiou, I., 2000. Recent history of salinity in Lake Pontchartrain. Fifth Bi-Annual Basics of the Basin Research Symposium, New Orleans, Louisiana. Abstract, pp. 35–36.

Kindinger, J.L.; Penland, S., and Williams, S.J., 2000a. A multidisciplinary synthesis of geology and geologic processes of Lake Pontchartrain, Louisiana. Fifth Bi-Annual Basics of the Basin Research Symposium, Abstracts with Program. (New Orleans, Louisiana, Pontchartrain Research Committee), pp. 45–47.

Kindinger, J.L.; Penland, S., and Williams, S.J., 2000b. USGS Lake Pontchartrain Cooperative Studies, 1994 to 1999. Fifth Bi-Annual Basics of the Basin Research Symposium. Abstracts with Program (New Orleans, Louisiana, Pontchartrain Research Committee), pp. 40–41.

Langmuir, D., 1997. *Aqueous Environmental Geochemistry*. Upper Saddle River, New Jersey: Prentice Hall, 600p.

Laxen, D.H.P. and Sholkovitz, E.R., 1981. Adsorption (coprecipitation) of trace metals at natural concentrations on hydrous ferric oxides in lake water samples. *Environmental Technology Letters*, 2, 561–568.

Lijklema, L., 1980. Interactions of orthophosphate with Fe(III) and aluminum hydroxides. *Environmental Science and Technology*, 14, 537–541.

Manheim, F.T. and Hayes, L., 2000. Geochemical and environmental relationships in sediments from Lake Pontchartrain and other southern Louisiana estuaries: results of comprehensive database development. Fifth Bi-Annual Basics of the Basin Research Symposium, New Orleans, Louisiana. Abstract, pp. 52–53.

Matheron, G., 1963. Principles of geostatistics. *Economic Geology*, 58, 1246–1266.

Poirrier, M.A., 1978. Studies of salinity stratification in southern Lake Pontchartrain near Inner Harbor Navigation Canal. *Louisiana Academy of Sciences*, 151, 26–35.

Poirrier, M.A.; Abadie, S.W., and Franze, C.D., 2000. Rangia clams as indicators of hypoxia in Lake Pontchartrain. Fifth Bi-Annual Basics of the Basin Research Symposium, Abstracts with Program. (New Orleans, Louisiana, Pontchartrain Research Committee), pp. 62–63.

Schurtz, M.H. and St. Pe, K.M., 1984. Water Quality Investigation of Environmental Conditions in Lake Pontchartrain. Report on Interim Findings to Louisiana Department of Environmental Quality, Water Pollution Division, 85p.

Signell, R.P. and List, J.H., 2002, Processes of Lake Pontchartrain circulation. *In:* Penland, S., Beall, A., and Kindinger, J. (eds.), *Environmental Atlas of the Lake Pontchartrain Basin*. New Orleans, Louisiana: Lake Pontchartrain Basin Foundation, U.S. Geological Survey Open File Report 002-206. CD-ROM available at http://pubs.usgs.gov/of/2002/of02-206/phy-environment/circulation.html (accessed September 16, 2009).

Sikora, W.B. and Sikora, J.P., 1982, Ecological Characterization of the Benthic Community of Lake Pontchartrain, Louisiana. Publ. No. LSU-CEL-81-18. U.S. Army Corps of Engineers, New Orleans District. Contract No. DSCW29-19-C-0099, 214p.

Swenson, E.M., 1980a. General hydrography of Lake Pontchartrain, Louisiana. *In:* Stone, J.H. (ed.), *Environmental Analysis of Lake Pontchartrain, Louisiana, Its Surrounding Wetlands, and Selected Land Uses*. Baton Rouge, Louisiana: CEL, CWR, LSU. Prepared for U.S. Army Corps of Engineers, New Orleans District, Contract No. DACW29-77-C-0253, pp. 57–155.

Swenson, E.M., 1980b. General hydrography of tidal passes of Lake Pontchartrain, Louisiana. *In:* Stone, J.H. (ed.), *Environmental Analysis of Lake Pontchartrain, Louisiana, Its Surrounding Wetlands, and Selected Land Uses*. Baton Rouge, Louisiana: CEL, CWR, LSU. Prepared for U.S. Army Corps of Engineers, New Orleans District, Contract No. DACW29-77-C-0253, pp. 157–217.

Turner, R.F.; Dortch, Q., and Rabalais, N.N., 1999, Effects of the 1997 Bonnet Carré opening on nutrients and phytoplankton in Lake Pontchartrain. Final report submitted to the Lake Pontchartrain Basin Foundation, 117 p.